frontiers | Frontiers in Materials

TYPE Original Research
PUBLISHED 19 September 2023
DOI 10.3389/fmats.2023.1218795

OPEN ACCESS

EDITED BY
Zhao Qin,
Syracuse University, United States

REVIEWED BY
Suvash Chandra Paul,
International University of Business Agriculture and Technology, Bangladesh
Ping Duan,
China University of Geosciences Wuhan, China
Denvid Lau,
City University of Hong Kong, Hong Kong SAR, China

*CORRESPONDENCE
Shihua Liang,
2112009005@gdut.edu.cn

RECEIVED 08 May 2023
ACCEPTED 06 September 2023
PUBLISHED 19 September 2023

CITATION
Zhang X, Zheng C, Xiong K, Yang K and Liang S (2023), Effect of fiber type and content on mechanical properties of microbial solidified sand.
Front. Mater. 10:1218795.
doi: 10.3389/fmats.2023.1218795

Effect of fiber type and content on mechanical properties of microbial solidified sand

Xiaogang Zhang[1], Chao Zheng[1], Kangwei Xiong[1], Kun Yang[1] and Shihua Liang[2]*

[1]Guangzhou Environmental Protection Investment Company Limited, Guangzhou, China, [2]School of Civil and Transportation Engineering, Guangdong University of Technology, Guangzhou, China

Fibers are applied to construction works to improve the strength and brittle failure of the soil. In this paper, fibers with a length of 6 mm are added to the microbial cemented sand, and fiber types and content are research variable. Unconfined compressive strength (UCS), permeability coefficient, water absorption rate, dry density, and calcium carbonate precipitation of the solidified sand were tested. The physical and mechanical properties of fiber types and content on the immobilization of microorganisms were also analyzed from the micro–macro perspective. Results are presented as follows. The UCS of the Microbial induced calcium carbonate precipitation (MICP) treated sand increases first and then decreases with the increasing fiber content. This phenomenon is due to the promotion of calcium carbonate precipitation by short fiber reinforcement, the limited movement of the sand particles caused by the formed network between the fibers, and the enhanced strength of the microbial solidified sand. However, the agglomeration caused by additional fibers leads to the uneven distribution of calcium carbonate and the reduction in strength. The optimum fiber contents of polypropylene, glass, polyvinyl alcohol, and basalt fibers are 0.4%, 0.2%, 0.2%, and 0.1%, respectively.

KEYWORDS

MICP, content of fibers, mechanical properties, type of fibers, $CaCO_3$ content

1 Introduction

Microbial-induced calcite precipitation (MICP) is an emerging and sustainable technology for soil improvement (Pacheco et al., 2022). This technology uses the reaction of metabolic products of microorganisms with calcium salts in the environment and rapidly precipitates calcium carbonate crystals with excellent cementation. As a popular direction of geotechnical engineering research, the influencing factors of microbial curing, such as temperature, curing method, particle size, nutrient composition, number of grouting, relative compactness of soil, pH value, oxygen supply, bacterial species and environmental factors (seawater, freshwater) have been deeply studied. Xiao et al. (2021) studied the influence of temperature on the solidified effect of MICP treatment, and found that the temperature affected the formation of $CaCO_3$ generated by MICP treatment. Zhao et al. (2014) pointed out that compared with the experimental factors the curing methods has a small influence on the solidified effect of MICP treatment. Song et al. (2022) found that the sand particle size has an important influence on the mechanical properties of the MICP treated sand. Yin et al. (2019) systematacially investigated the influence of nutrient composition, number of grouting, bacterial species and pH value on the solidified effect

of MICP treatment. Kim et al. (2014) pointed out that the relative compactness of soil greatly affected the UCS of the MICP treated sand. Li et al. (2018) investigated the effects of oxygen supply on MICP treatment catalyzed by sporosarcina pasteurii and found that a sufficient air supply is essential to improve MICP processes catalyzed by aerobic bacteria. Peng et al. (2022) conducted a MICP aqueous solution experiment to investigate the influence of the seawater and freshwater on the relationship between calcium carbonate precipitation and time, and found that The UCS in the freshwater environment were approximately 30%–45% higher than those in the seawater environment. Previous studies have shown that the mechanical properties of MICP-treated sand samples are substantially improved (Chi et al., 2022). However, as the durability of building materials becomes more important (Peng et al., 2023), the uneven distribution of calcium carbonate and the brittle destruction characteristic (Zhao et al., 2020; Wang et al., 2022) are remarkable shortcomings of MICP treated sand, which limit the promotion of the MICP technology.

In this regard, many researchers have combined fiber reinforcement and MICP techniques, which can effectively improve the brittle damage characteristics of soils. Among them, Xie et al. (2019) found that fiber incorporation in MICP treated sand, in which different mass fractions of 12 mm polypropylene fibers are incorporated in quartz river sand, can markedly improve the unconfined compressive and residual strengths of soil samples and remarkablely enhance the toughness of soil samples when damaged, yielding optimal fiber incorporation of 0.15%. Li et al. (2016) investigated the fiber content on microbially cured Ottawa sand. Their results showed that the addition of fibers to MICP-treated sand significantly improved the shear strength, ductility, and breaking strain. Choi et al. (2016) found that the incorporation of polyvinyl alcohol fibers with different fiber contents in microbially cured Ottawa silica sand effectively improved the unconfined compressive and splitting tensile strengths of the cured sand and enhanced its brittleness. Deng et al. (Ke et al., 2019) concluded that fiber type and fiber doping are important factors affecting the strength and deformation of fiber-reinforced soils in exploring the current research state on fiber-reinforced soils. At present, the researches focus on the influence of a single type of fiber with different content on the UCS of the MICP treated sand. However, different types of fibers have different surface morphologies, physical and mechanical properties (Feng et al., 2023a; Feng et al., 202b), and have different influence on the other physical and mechanical properties (such as water absorption and permeability) of the MICP treated fiber reinforced sand. This is not studied systematacially and in depth. Therefore, various physical and mechanical tests were conducted on the MICP treated sand collaborating four types of fibers with different contents to investigate the strengthening mechanism of different types of fibers for solidifying the MICP treated sand.

It is reported that adding 0.1%–2.5% various types of fibers is capable of improving the mechanical strength of solidified soils (Kumar et al., 2006; Tang et al., 2012; Liang et al., 2018; Gui et al., 2022) and the optimal dosage of fiber content ranging from 0.15% ~0.25% for MICP treated sand (Zheng et al., 2019a). In this regard, the fiber doses of 0%, 0.1%, 0.2%, and 0.4% and the fiber types of polypropylene, glass, polyvinyl alcohol, and basalt fibers were selected in this paper as the research objects to study the effect of fibers on the physical and mechanical properties of the MICP treat sand. The MICP treated sand without fiber was used as a control test.

2 Test materials

2.1 Experimental bacteria

Previous studies have demonstrated that the *bacillus* sporosarcina pasteurii, which is poisonless and harmless, is commonly used and effective in MICP treatment (Mondal and Ghosh, 2019). Therefore, the *bacillus* sporosarcina pasteurii was adopted in the present work and purchased from the Netherlands (DSM company, No. DSM33). An expanded culture of bacteria was prepared. The culture solution comprised the following: 20 g/L of yeast extract, 10 g/L of ammonium sulfate, and 2 g/L of sodium hydroxide. 50 mL of bacteria was used for each round of each sample.

2.2 Test fibers

The fibers used in the present work are polypropylene, glass, polyvinyl alcohol, and basalt fibers with a length of 6 mm, which are purchased from Haining Anjie Materials Company in Jiangsu province, China. The physical properties of the four types of fibers that are provided by the manufacturers are shown in Table 1, and the pictures of these fibers are shown in Figure 1.

2.3 Preparation of nutrient solution

Each liter of nutrient solution in this experiment comprised the following: $NaHCO_3$ (2.12 g), $CaCl_2$ (55.50 g), NH_4Cl (10 g), nutrient broth (3 g), and urea (30 g). The specific steps of nutrient solution injection are as follows. Bacterial and nutrient solutions were injected into the specimens by a peristaltic pump. According to the research of Lian et al. (2021) 2~3 rounds of bacterial and nutrient solutions injection for MICP treated sand can reach an efficient solidification effect. Therefore, the MICP treated fiber reinforced sand sample was conducted by two rounds of grouting to form a homogeneous MICP treated sample: each round of grouting lasted nine times, and each grouting interval was 8 h. The solutions were left to stand after the first round of grouting was completed, and the bacterial solution was injected again for the second round. Each specimen was injected with 50 mL of nutrient solution each time.

2.4 Test sand

It is reported that poor grading sand is commonly used, and can achieve good solidification effect by MICP treatment (Zheng et al., 2019b; Chen et al., 2021a; Chen et al., 2023). Therefore, the test was conducted using Fujian ISO standard sand, which is a fine sand with uniform soil particles and poor grading, with a specific gravity of test sand G_s = 2.653. The average particle size of sand was smaller than 10%: D_{10} = 0.282, D_{30} = 0.437, D_{50} = 0.821, andD_{60} = 1.083. The unevenness factor C_u = 3.840 and the curvature factor C_c = 0.625; a large inhomogeneity coefficient C_u indicates a wide grain group distribution of the sand. The grading size of the Fujian ISO standard sand is shown in Figure 2.

TABLE 1 Physicomechanical behaviors of fibers.

Type	Density ρ/(g/cm^3)	Line density/tex	Diameter/mm	Tensile strength/MPa	Elastic modulus/MPa	Breaking elongation/%
Polypropylene	0.91	—	0.025	≥500	≥3,850	2.3
Glass	2.699	4,897	0.0174	2,180	8,720	2.52
Polyvinyl alcohol	1.29	—	0.01509	1830	40,000	6.9
Basalt	—	2,392	—	3,836	62,000	3.0

FIGURE 1
Physical picture of the fibers: **(A)** Polypropylene fibers; **(B)** Glass fibers; **(C)** Polyvinyl alcohol fibers; **(D)** Basalt fibers.

A PVC pipe with an inner diameter of 39.1 mm and a height of 115 mm was used to prepare the specimens, and the specimen size was computed as follows: diameter × height = 39.1 mm × 80 mm, which is recommended by the specification of soil test (GB/T50123—2019) (Author Anonymous, 2019) for the sample with soil particle size not larger than 2.0 mm. The ratio of the maximum particle size (2.0 mm) of the sample to the diameter of the sample is 1/10, therefore, the particle size effect can be avoided (Feng and Fang, 2016; Liang et al., 2023). Three parallel specimens were prepared for each of the test groups.

2.5 Sample preparation

When preparing the MICP treated fiber reinforced sand samples, the specified amount of fibers was added into the host sand in four batches, after each batche, the fibers and sand particles were mixed thoroughly to ensure that the fibers were uniformly distributed in the host sand. The sand-fiber mixture was then loaded in the mold by hammering method (Diambra et al., 2010). The control dry density of each MICP treated fiber reinforced sand samples was 1.4 g/cm^3. The schematic diagram of the MICP treated fiber reinforced sand sample preparation is shown is Figure 3.

3 Experimental test methods

The treated sand samples were subjected to water absorption, dry density, porosity, calcium carbonate content, permeability coefficient, unconfined compressive strength and SEM (scanning electron microscope) tests. Here, the water absorption, dry

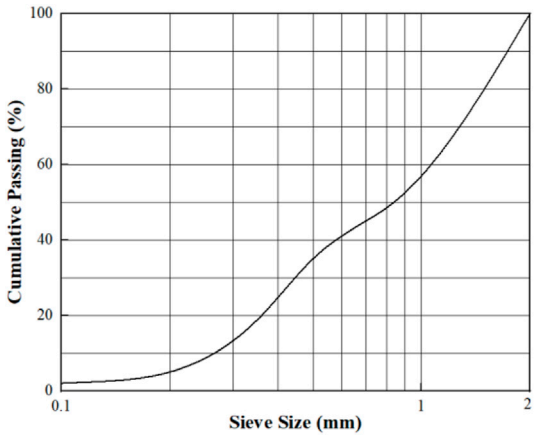

FIGURE 2
Grading size of the Fujian ISO standard sand.

density and porosity are important physical properties of the MICP treated fiber reinforced sand sample, the permeability coefficient and unconfined compressive strength are important mechanical properties of the MICP treated fiber reinforced sand sample, and the calcium carbonate content has a key influence on the physical and mechanical properties of the MICP treated fiber reinforced sand sample. Therefore, the aforementioned parameters are determined in the present work. The specific test scheme is shown in Table 2. All these tests were conducted according to the specification of soil test (GB/T50123—2019) (Author Anonymous, 2019).

3.1 Determination of permeability coefficient

The cured specimen is first placed into the mold. The water injection is opened and the water clip is stopped. Water injection runs through the head tube to the mold. The water level ranges from 70 to 170 cm during the test. The water injection stop clip is closed when water through the specimen comes out of a certain time. The initial height of the head tube and time are recorded and the same certain time interval is taken. The head tube height is also recorded. The permeability coefficient is obtained on the basis of Eq. 1 (Author Anonymous, 2019).

$$k_T = 2.3\frac{aL}{A(t_2 - t_1)}log\frac{H_1}{H_2} \quad (1)$$

where K_T is the permeability coefficient of the MICP treated fiber reinforced sand sample; a is the cross-sectional area of the variable head tube; A and L are the cross-sectional area and height of the MICP treated fiber reinforced sand sample; 2.3 is the "In" and log of the transformation factor; H_1 and H_2 are the starting and ending heads, respectively; t_1 and t_2 are the starting and ending times of the measured head, respectively.

3.2 Determination of water absorption

First, the cured sand column is dried and its mass M_1 is weighed. The dried sand column is then soaked in water for 24 h. The sand column and the residual water on the surface of the sand column are quickly removed and its mass M_2 is weighed. The water absorption rate is finally obtained in accordance with Eq. 2.

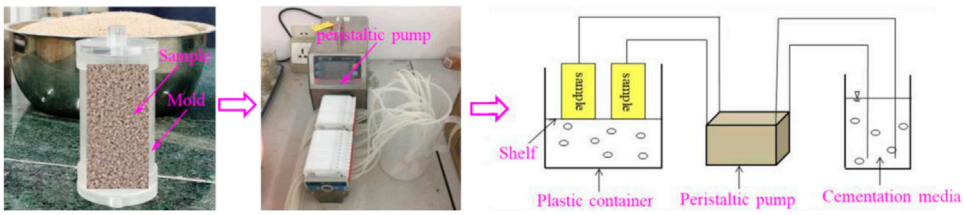

FIGURE 3
The schematic diagram of the MICP treated fiber reinforced sand sample preparation.

TABLE 2 The specific test scheme.

Test group	Fiber type	Fiber length/mm	Fiber content/%	Test type
1	Polypropylene	6	0, 0.1, 0.2, 0.4	calcium carbonate content, permeability, water absorption rate, porosity rate, dry density and UCS
2	Glass	6	0, 0.1, 0.2, 0.4	calcium carbonate content, permeability, water absorption rate, porosity rate, dry density and UCS
3	Polyvinyl alcohol	6	0, 0.1, 0.2, 0.4	calcium carbonate content, permeability, water absorption rate, porosity rate, dry density and UCS
4	Basalt	6	0, 0.1, 0.2, 0.4	calcium carbonate content, permeability, water absorption rate, porosity rate, dry density and UCS

$$\omega = \frac{M_2 - M_1}{M_1} \times 100\% \quad (2)$$

where w is the water absorption rate of the MICP treated fiber reinforced sand sample; M_1 is the mass of the dry MICP treated fiber reinforced sand sample; M_2 is the mass of the MICP treated fiber reinforced sand sample after soaking in water for 24 h.

3.3 Determination of porosity

The porosity of the MICP treated fiber reinforced sand sample was determined by the drying method, and the porosity was calculated in accordance with Eq. 3.

$$n = \frac{M_1 - M_2}{\rho_w V} \times 100\% \quad (3)$$

where n is the porosity of the MICP treated fiber reinforced sand sample; ρ_w is the density of water at 4°C; V is the volume of the MICP treated fiber reinforced sand sample.

3.4 Determination of dry density

Dry density is calculated using Eq. 4.

$$\rho_d = \frac{M_2}{V} \quad (4)$$

where ρ_d is the dry density of the MICP treated fiber reinforced sand sample.

3.5 Determination of calcium carbonate content

After taking the damaged sample, the mass of calcium carbonate was determined by acid washing test. Before pickling, the mass was measured by drying and recorded as M_1. The specimen was then placed in a beaker and dissolved by adding excess hydrochloric acid. When the specimen in the beaker was free of lumpy particles and bubbles, the calcium carbonate was considered to be completely reacted, and the dissolved sand was rinsed with water several times. The rinsed sand was then dried in an oven to a constant weight and weighed and recorded as M_2 mass (Ma et al., 2021). The amount of calcium carbonate generated is calculated in accordance with Eq. 5.

$$M_{(C_aCO_3)} = \frac{M_1 - M_2}{M_1} \times 100\% \quad (5)$$

3.6 Unconfined compressive strength

The unconfined compressive strength is loaded by the liquid crystal automatic pressure equipment (YAW-S300) until the specimen is destroyed (Da et al., 2016; Chen et al., 2021b), and the peak compressive strength is taken as the unconfined compressive strength of the sample q_u. The loading strain rate was 1%/min. The measurement system of the equipment consisted of a displacement transducer, load transducer, and recorder. The acquisition system connected to a computer displayed and recorded all the stress-strain curves of the loading procedure.

3.7 SEM test

The samples after UCS tests were quenched with anhydrous ethanol to prevent further reactions (Chen et al., 2022), dried in an oven at 65°C for 24 h, and then ground with a mortar. The appropriate size specimen is taken for SEM test by using a ZEISS Sigma 500/VP field emission scanning electron microscope. Besides, the elements of typical sample is determined by energy dispersive spectrometer (EDS). Gold is then sprayed on the specimen and placed in the vacuum chamber of the scanning electron microscope. A typical spot is selected to shoot ×500 magnification.

This section may be divided by subheadings. It should provide a concise and precise description of the experimental results, their interpretation, as well as the experimental conclusions that can be drawn.

4 Results and discussion

4.1 The $CaCO_3$ content, water absorption rate, porosity rate and dry density of the MICP treated fiber reinforced sand samples

The $CaCO_3$ content, water absorption rate, porosity rate and dry density of the MICP treated fiber reinforced sand samples were shown in Figure 4.

It is apparent from Figure 4 that the calcium carbonate content of the MICP treated sand samples increased compared with that of the control group with 0% fiber content, and the amount of calcium carbonate precipitation demonstrated a trend of first increasing and then decreasing with the increase in fiber content. The calcium carbonate content of the MICP treated sand samples increases by 21%, 12%, 28% and 8%, respectively for polypropylene, glass, polyvinyl alcohol, and basalt fibers with the optimal dosage. It is noted that different types of fibers have different surface characteristics and dispersibility, which affects the adhering of the calcium carbonate precipitation on the fibers, and then has an influence on the formation of the calcium carbonate precipitation. Therefore, the amount of calcium carbonate precipitation is associated with the activity of the bacteria, and the bacteria readily adhere to the fibers, leading to an increase in the calcium carbonate precipitation. The water absorption rate and porosity rate of the MICP treated fiber reinforced sand samples decreased compared with that of the control group with 0% fiber content, when 0.1% glass, polyvinyl alcohol and basalt fibers was added. The water absorption, and porosity decreased and the dry density of the MICP treated sand samples increased after the addition of fibers. The calcium carbonate content of the MICP treated fiber reinforced sand samples with the same fiber content

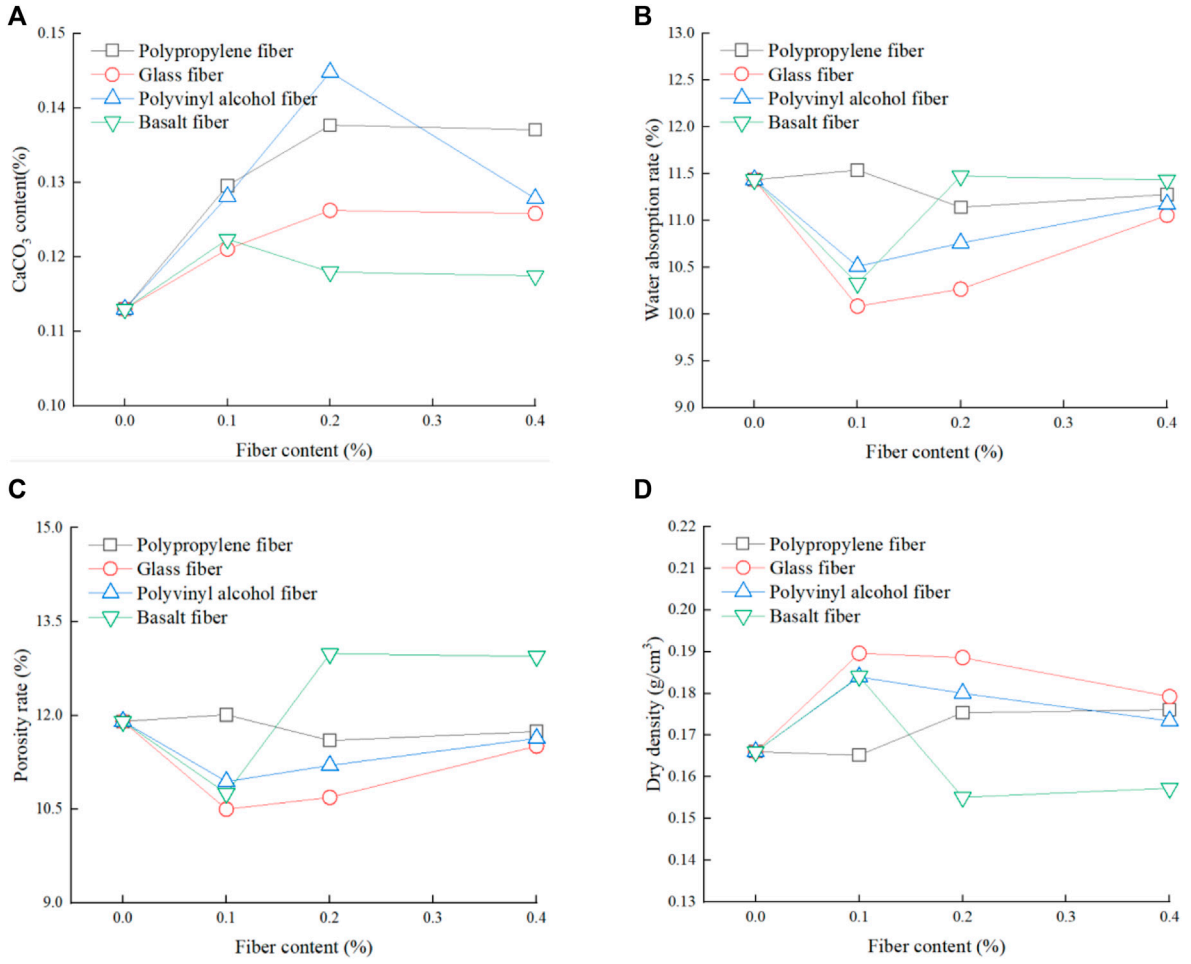

FIGURE 4
Physical properties of the MICP treated fiber reinforced sand samples: **(A)** $CaCO_3$ content; **(B)** Water absorption rate; **(C)** Porosity rate; **(D)** Dry density.

was negatively correlated with the water absorption rate and porosity rate, and positively correlated with the dry density.

The increase in calcium carbonate content of the MICP-treated sand samples with the addition of fibers was due to the uniform dispersion of fibers in the sand samples. Such a dispersion provided additional "landing sites" for bacteria when they "flowed" through the sand column, effectively retaining additional bacteria to promote the production of calcium carbonate precipitation (Xie et al., 2019). Above a certain amount of fibers, the decrease in calcium carbonate content with increasing fiber content is due to the insufficient mixing or even agglomeration of excess fiber during sample preparation. This phenomenon changes the "nucleation sites" for microbial curing and directly affects the location and amount of calcium carbonate production (Li et al., 2016).

4.2 Mechanical properties

(1) Permeability of the MICP treated fiber reinforced sand samples

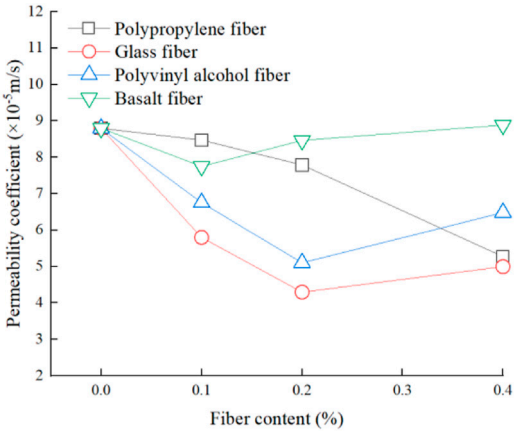

FIGURE 5
Permeability coefficient of the MICP treated fiber reinforced sand samples.

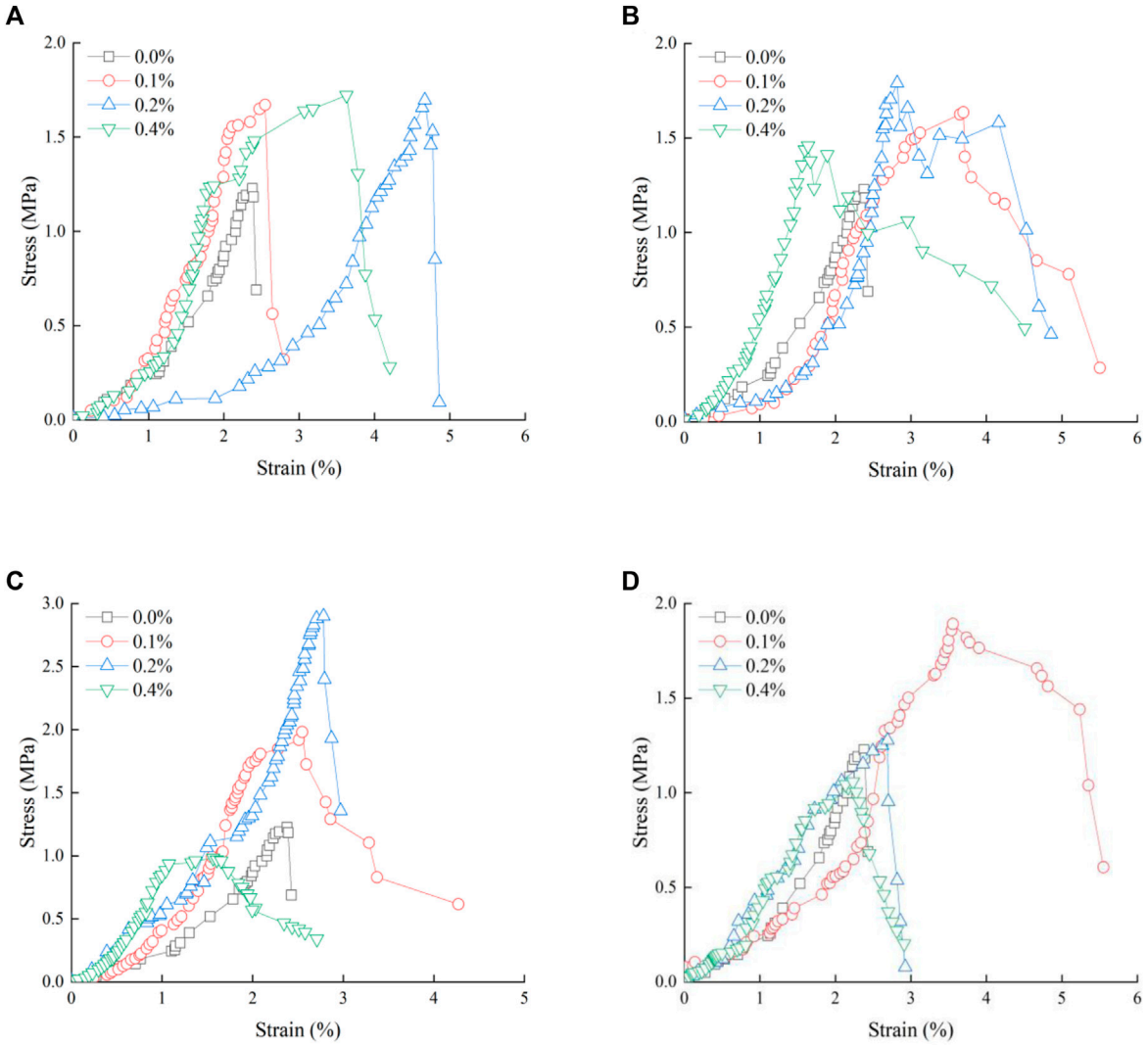

FIGURE 6
Unconfined compressive stress–strain diagrams of the MICP treated fiber reinforced sand samples for different types of fibers: **(A)** Polypropylene fiber; **(B)** Glass fiber; **(C)** Polyvinyl alcohol fiber; **(D)** Basalt fiber.

The permeability coefficient of the MICP treated fiber reinforced sand samples is shown in Figure 5. It is apparent from Figure 5 that a certain amount of fibers is capable of reducing the permeability of the MICP treated sand. In the case of the MICP treated sand samples collaborating glass, polyvinyl alcohol and basalt fibers, the permeability coefficient of the samples decreases first and then increases with an increase in fiber content. While for the MICP treated sand samples collaborating polypropylene fibers, the permeability coefficient of the samples decreases with an increase in fiber content. Glass fibers has the best effect on reducing the permeability of the MICP treated sand sample, and the optimal fiber dosage is 0.2%. The reason for the aforementioned phenomenon is that the fibers fill the pores of the sand particles and the $CaCO_3$ generated by the MICP treatment is promoted, so that the porosity of the sand sample is greatly reduced, leading to a reduction of the permeability coefficient of the MICP treated fiber reinforced sand samples. As the addition of fibers becomes excessive, some of the fibers intersect each other to form a preponderant seepage channel between the contacting fibers, resulting in an increase in the permeability of the MICP treated fiber reinforced sand samples.

(2) Unconfined compressive strength (UCS)

The stress-strain relationships and UCS of the MICP treated fiber reinforced sand samples are shown in Figures 6, 7, respectively. Each stress-strain curve and UCS of the samples in the figure is determined by the average of the results of the three parallel tests in the same test group.

Figure 6 shows that the addition of fibers can significantly improve the unconfined compressive strength of the MICP treated samples. The unconfined compressive strength of the control group of the MICP treated sand samples without additional fibers was 1.23 MPa. Compared with the UCS of the control group, the UCS of the MICP treated **polypropylene fiber**

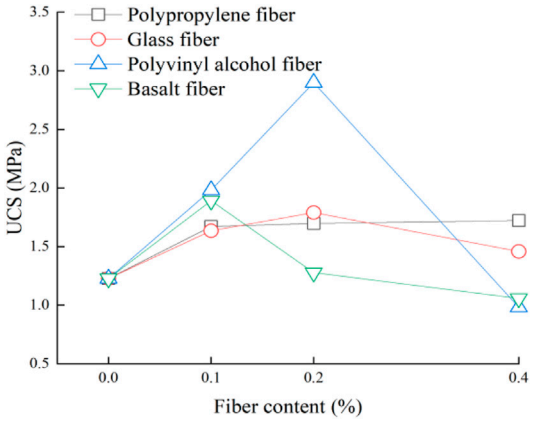

FIGURE 7
Unconfined compressive strength of the MICP treated fiber reinforced sand samples.

reinforced sand samples increased by 36%, 38% and 40%, respectively for fiber content of 0.1%, 0.2% and 0.4%; the UCS of the MICP treated **glass fiber** reinforced sand samples increased by 33%, 46% and 19%, respectively for fiber content of 0.1%, 0.2% and 0.4%; the UCS of the MICP treated **polyvinyl alcohol fiber** reinforced sand samples increased by 61% and 136%, respectively for fiber content of 0.1% and 0.2%; and the UCS of the MICP treated **basalt fiber** reinforced sand samples increased by 54% and 4%, respectively for fiber content of 0.1% and 0.2%.

In the case of concerning the enhancement of the UCS, the optimal fiber admixture corresponds to 0.4%, 0.2%, 0.2%, and 0.1%. The UCS increases first and then decreases with rising fiber content. The strength increases because the uniformly distributed fibers in the sand sample can retain additional bacteria to promote the generation of calcium carbonate precipitation (Xie et al., 2019). The calcium carbonate adheres to the surface of the fibers, increasing the roughness of the fiber surface, strengthening the interfacial friction between the fibers and the sand (Yin et al., 2019), restraining the lateral movement of the sand, and raising the stiffness of the sand sample. The three-dimensional mesh structure formed between the fibers and strengthened the integrity of the sand sample (Zheng et al., 2019a), thus increasing the strength of the sand sample. The excessively high fiber content resulted in strength reduction, easily forming clumps between fibers. This phenomenon complicates the even mixing with the sand sample, which directly affects the distribution of calcium carbonate and leads to the reduction in effective calcium carbonate content (Al Imran et al., 2020) and strength. The uneven distribution of fibers in the sand column also leads to the emergence of a weak interface of force inside the sand column and the reduction in unconfined compressive strength. Overall, the results reveal an optimal fiber content value for the MICP treated fiber reinforced sand samples.

The stress–strain curve in Figure 6B shows that the stress of the MICP treated sand sample without the addition of fiber reaches its peak and then sharply drops, which is typical of brittle damage. By contrast, when the microbial consolidation sand column was damaged by adding fiber, a "small peak" decline was observed; additional fiber content leads to an increased number of "small peaks." When the specimen is damaged, cracks appear inside and the fibers between the cracks can bear the extra load and inhibit crack development, resulting in the stress–strain curve with a rising pattern after the peak. With a further increase in specimen strain, some fibers are pulled out or off and cracks are further developed, which, in turn, leads to a sudden decrease in stress. However, the cracks develop again and the other fibers continue to carry the tensile stress, resulting in another rising "hill." A high fiber content indicates the presence of a high number of fibers between cracks, demonstrating evident inhibition of crack development by fibers. The results show that the short fiber reinforcement can change the brittle damage mode to ductile damage mode in MICP-treated sand samples.

Figure 7 shows that different fiber types and contents have varying curing effects on MICP-treated sand, and the effect of fiber content on microbial curing sand is more intense than that of fiber type. It is apparent from Figure 7 that the increase in the UCS of the MICP-treated sand from fiber addition weakens after reaching a certain amount of fiber dosage. For instance, with the increase of the polyvinyl alcohol fiber content ranging from 0.0% to 0.2%, the UCS of the MICP treated fiber reinforced sand sample increases from 1.24 to 2.92 MPa. However, its UCS reduces to 1.02 MP when the polyvinyl alcohol fiber content reaches 0.4%. Compared with the UCS of the control sample, the UCS of the MICP treated sand sample cooperated with 0.2% polyvinyl alcohol fiber is increased by 136%. The fibers distributed in the host sand that covered with Calcium carbonate precipitation restrict the relative displacement of sand particles in the sample, which connects the dispersive sand particles together and improves the UCS of the MICP treated sand. However, with excessive fiber contents, more calcium carbonate precipitation attracted to be adhered to fiber surface rather than the sand particles, and consequently reduces the cementitious effect between sand particles, leading to weaker UCS of the MICP treated fiber reinforced sand sample (Li et al., 2016). Moreover, the anchoring effect of the fiber has an important influence on the permeability and strength of the MICP treated fiber reinforced sand samples (Xie et al., 2019). Different types of fibers have different dispersibility and adsorbability (Zheng et al., 2023), which have an influence on the formation and location of the calcium carbonate, and then affect the permeability and strength of the MICP treated fiber reinforced sand samples.

Different types of fibers have various surface physical properties, which will lead to different forms of contact between the fiber surface and the soil: a high surface roughness strengthens the interfacial friction between fibers and sand particles (Liang et al., 2022). The fiber content directly affects the three-dimensional mesh structure formed between fibers: additional fiber roots lead to a large contact area between fibers and sand particles, revealing a significant frictional effect in the MICP treated sand. It is noted that the strength of the four types of fibers is much higher than that of the MICP treated sand. In this regard, four types of fibers have an important on the solidifying effect of MICP treated sand, and fiber content has a more substantial effect than fiber type, and the polyvinyl alcohol fiber curing sand mixed with a 0.2% fiber ratio has the best effect.

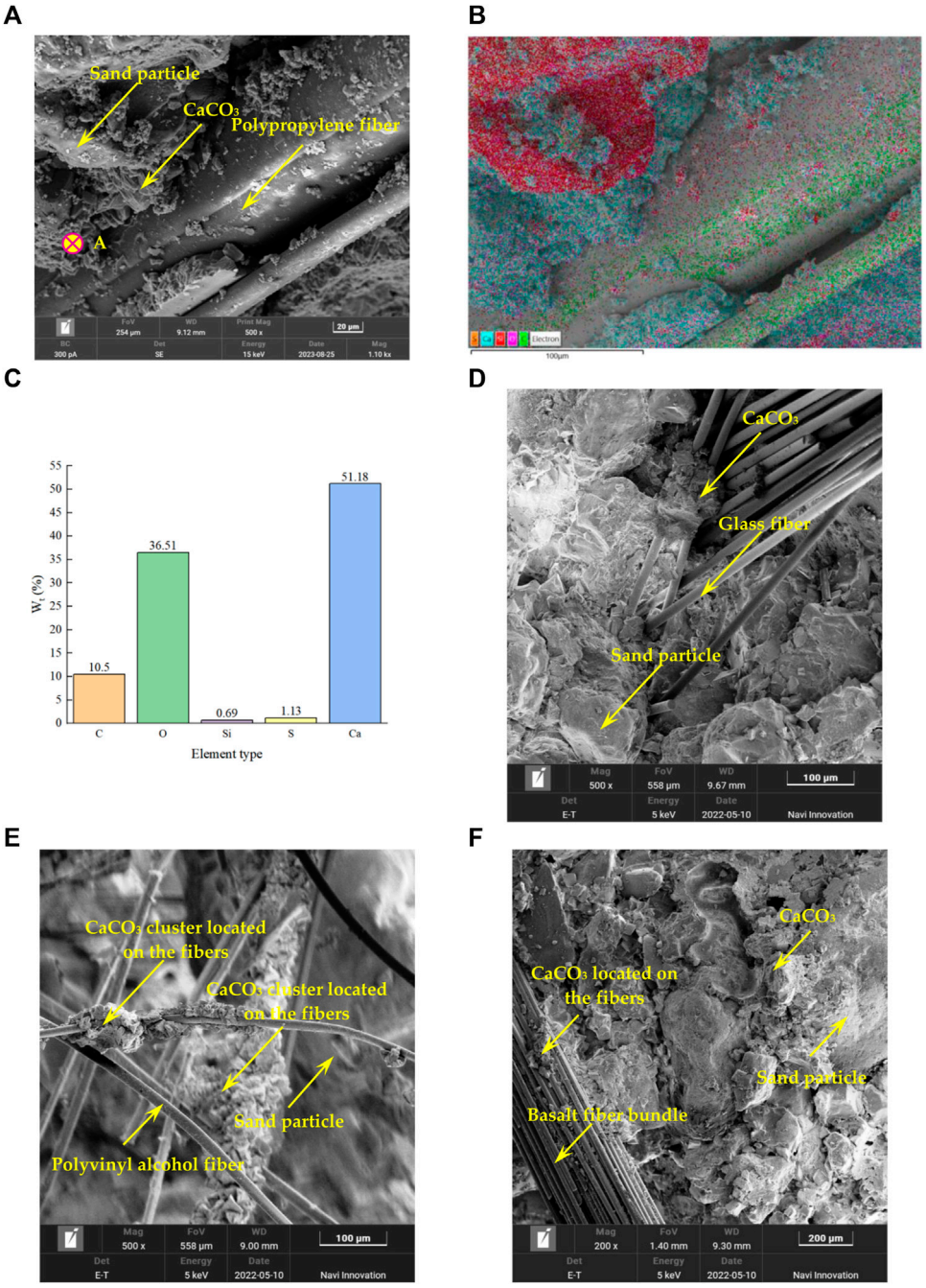

FIGURE 8
The SEM images and EDS result of typical MICP treated sand collaborating fibers: **(A)** SEM-Polypropylene fiber; **(B)** EDS-surface scan-Polypropylene fiber; **(C)** EDS-point A scan-Polypropylene fiber **(D)** SEM-Glass fiber; **(E)** SEM-Polyvinyl alcohol fiber; **(F)** SEM-Basalt fiber.

4.3 Microstructure

The microstructure of the MICP treated sand collaborating different types of fibers were shown in Figure 8.

Figure 8 shows that calcium carbonate is attached to the surface and pores of the fibers and sand particles, the fibers span between the sand particles, and the joints are bonded by calcium carbonate. Therefore, the fibers strengthen the MICP cementation through bridging action.

It is apparent from Figures 8A, D that some of the polypropylene and glass fibers intersected each other, which decreased the friction effect between the fibers and sand particles, and just a few precipitation located on the fibers. According to Figures 8B, C that the elements of the cluster-like precipitation around the fiber and those of point A in this precipitation were Ca (blue points), C (green points) and O (purple points), indicating that this cluster-like precipitation was $CaCO_3$. In the case of Figure 8E, the distribution of polyvinyl alcohol fibers is dispersive and large amount of $CaCO_3$ was

located on these fibers, leading to an enhancement of the friction effect and bridging effect between the fibers and sand particles. For Figure 8F, the basalt fibers tended to form fiber bundles, which had a negative impact on the adhesion of $CaCO_3$ on the fibers. These results are in accordance with the macro test results of the calcium carbonate, UCS of the MICP treated fiber reinforced sand samples shown in Figure 4A and Figure 7, respectively. Moreover, the calcium carbonate generated on the fiber surface further strengthens its roughness to increase the interfacial friction. The fibers at the fracture surface can bear part of the load and inhibit the development of cracks, thus improving the brittle damage characteristics of MICP. The presence of fibers simultaneously provides additional nucleation sites for bacteria, which leads to an increase in the effective calcium carbonate content inside the sand column, an increase in the cementation level, and a subsequent rise in compressive strength.

5 Conclusion

(1) In the case of MICP treated sand, a small amount of fiber is capable of effectively increasing the formation of calcium carbonate precipitation. The amount of calcium carbonate precipitation is negatively correlated with the permeability coefficient, water absorption and porosity, and positively correlated with the dry density with the same fiber content.
(2) The fiber content has an important influence on the mechanical properties of MICP treated sand. The unconfined compressive strength of the MICP treated fiber reinforced sand increase first and then decrease with an increase in fiber content. The optimum fiber content of polypropylene, glass, polyethylene, and basalt fibers are 0.4%, 0.2%, 0.2%, and 0.1%, respectively.
(3) Four types of fibers have an important on the solidifying effect of MICP treated sand, and fiber content has a more substantial effect than fiber type.

Finally, it is noted that this paper is a preliminary investigation of the influence of different types and contents of fibers on the physical and mechanical properties of the MICP treated sand, a total of 16 groups of tests were conducted. However, the optimum fiber content is also influenced by fiber length, sand particle size and relative density and the MICP treatment procedure, more specific and systematic experimental studies are recommended in the future. Moreover, advanced microscopic test technique such as CT (computerized tomography) technique is expected to reconstruct the three dimensional distribution of the fibers and calcium carbonate in the MICP treated fiber reinforced sand sample to investigate the solidification mechanism of MICP treatment collaborating fibers.

Data availability statement

The data analyzed in this study is subject to the following licenses/restrictions: The data used to support the findings of this study are available from the corresponding author upon request. Requests to access these datasets should be directed to SL, 2112009005@gdut.edu.cn.

Author contributions

Conceptualization, SL; Writing, KY; Formal analysis, KY; methodology, CZ; software, KX; data curation, XZ. All authors contributed to the article and approved the submitted version.

Funding

This paper was funded by the National Natural Science Foundation of China (General Program) (grant number 52078142), National Natural Science Foundation of Guangdong (grant number 2022A1515011047), and the Science and Technology Program of Guangzhou, China (grant number 202002030194).

Acknowledgments

We thank EssayStar (http://essaystar.com/) for its linguistic assistance during the preparation of this manuscript.

Conflict of interest

Authors XZ, CZ, KX, and KY were employed by Guangzhou Environmental Protection Investment Company Limited.

The remaining author declares that the research was conducted in the absence of any commercial or financial relationships that could be construed as a potential conflict of interest.

Publisher's note

References

Al Imran, M., Gowthaman, S., Nakashima, K., and Kawasaki, S. (2020). The influence of the addition of plant-based natural fibers (jute) on biocemented sand using MICP method. *Materials* 13, 4198. doi:10.3390/ma13184198

Chen, H. G., Chow, C. L., and Lau, D. (2022). Recycling used engine oil in concrete: fire performance evaluation. *J. J. Build. Eng.* 64, 105637. doi:10.1016/j.jobe.2022.105637

Chen, H. G., Qin, R. Y., Chow, C. L., and Lau, D. (2023). Recycling thermoset plastic waste for manufacturing green cement mortar. *Cem. Concr. Compos.* 137, 104922. doi:10.1016/j.cemconcomp.2022.104922

Chen, H. G., Qin, R. Y., and Lau, D. (2021a). Recycling used engine oil in concrete design mix: an ecofriendly and feasible solution. *J. Clean. Prod.* 329, 129555. doi:10.1016/j.jclepro.2021.129555

Chen, H. G., Yang, J. J., and Chen, X. H. (2021b). A convolution-based deep learning approach for estimating compressive strength of fiber reinforced concrete at elevated temperatures. *Constr. Build. Mater.* 313, 125437. doi:10.1016/j.conbuildmat.2021.125437

Chi, L., Lei, T., Caihuan, D., Yongfeng, Z., and Yanxing, W. (2022). Experimental study of MICP technology combined with porous silica adsorbent material for the

remediation of Zn-Pb composite contaminated soil solidification/stabilization. *Geotechnics* 43, 307–316. doi:10.16285/j.rsm.2021.1403

Choi, S. G., Wang, K. J., and Chu, J. (2016). Properties of biocemented, fiber reinforced sand. *Constr. Build. Mater.* 120, 623–629. doi:10.1016/j.conbuildmat.2016.05.124

Da, B., Yu, H., Ma, H., Tan, Y., Mi, R., and Dou, X. (2016). Experimental investigation of whole stress-strain curves of coral concrete. *Constr. Build. Mater.* 122, 81–89. doi:10.1016/j.conbuildmat.2016.06.064

Diambra, A., Ibraim, E., Wood, D. M., and Russell, A. R. (2010). Fibre reinforced sands: experiments and modelling. *Geotext. geomembranes* 28 (3), 238–250. doi:10.1016/j.geotexmem.2009.09.010

Feng, D. L., and Fang, Y. G. (2016). Theoretical analysis and experimental research on multiscale mechanical properties of soil. *Int. J. Geomechanics* 16 (4), 04015094. doi:10.1061/(asce)gm.1943-5622.0000573

Feng, D. L., Wang, Y. X., and Liang, S. H. (2023a). Theoretical and experimental study on multiscale coupled Mohr–Coulomb shear strength criterion of fibre-reinforced sand. *Undergr. Space*, 26. doi:10.1016/j.undsp.2023.05.008

Feng, D. L., Wang, Y. X., and Liang, S. H. (2023b). A mechanism-based shear strength theoretical model for fiber-reinforced cemented soil. *J. Eng. Mech.* 149 (2), 04022108. doi:10.1061/jenmdt.emeng-6835

Gui, Y., Wong, W. Y., and Gallage, C. (2022). Effectiveness and sensitivity of fiber inclusion on desiccation cracking behavior of reinforced clayey soil. *Int. J. geomechanics* 22 (3), 06021040. doi:10.1061/(asce)gm.1943-5622.0002278

Ke, D., Kai, W., Yeqiu, L., Yi, Y., Meihuan, H., and Xiaohua, X. (2019). Status and progress of research on fiber modified soil. *Guangdong Chem. Ind.* 46, 112–113. doi:10.3969/j.issn.1007-1865.2019.13.054

Kim, D., Park, K., and Kim, D. (2014). Effects of ground conditions on microbial cementation in soils. *Materials* 7, 143–156. doi:10.3390/ma7010143

Kumar, A., Walia, B., and Mohan, J. (2006). Compressive strength of fiber reinforced highly compressible clay. *Constr. Build. Mater.* 20 (10), 1063–1068. doi:10.1016/j.conbuildmat.2005.02.027

Li, M. D., Li, L., Ogbonnaya, U., Wen, K. J., Tian, A. G., and Amini, F. (2016). Influence of fiber addition on mechanical properties of MICP-treated sand. *J. Mater. Civ. Eng.* 28, 10. doi:10.1061/(asce)mt.1943-5533.0001442

Li, M. D., Wen, K. J., Li, Y., and Zhu, L. P. (2018). Impact of oxygen availability on microbially induced calcite precipitation (MICP) treatment. *Geomicrobiol. J.* 35, 15–22. doi:10.1080/01490451.2017.1303553

Liang, S. H., Xiao, X. L., Li, Z., and Feng, D. L. (2021). Effect of nutrient solution composition on bio-cemented sand. *Crystals* 11, 1572. doi:10.3390/cryst11121572

Liang, S. H., Xiao, X. L., and Feng, D. L. (2023). Study on large-scale direct shear test on soil–rock mixture in an immersion state under water. *Int. J. Geomechanics* 23 (2), 04022294. doi:10.1061/ijgnai.gmeng-7643

Liang, S., Niu, J., Liu, S., et al. (2018). Effect of polypropylene fiber content on strength properties of cement soil. *Build. Sci.* 34 (3), 90–96. doi:10.13614/j.cnki.11-1962/tu.2018.03.014

Liang, S. H., Xiao, X. L., Wang, J., Wang, Y. X., Feng, D. L., and Zhu, C. Y. (2022). Influence of fiber type and length on mechanical properties of MICP-treated sand. *Materials* 15, 4017. doi:10.3390/ma15114017

Ma, G. L., He, X., Jiang, X., Liu, H. L., Chu, J., and Xiao, Y. (2021). Strength and permeability of bentonite-assisted biocemented coarse sand. *Can. Geotech. J.* 58, 969–981. doi:10.1139/cgj-2020-0045

Author Anonymous. *Ministry of water Resources of the people's Republic of China*. Geotechnical Test Method Standards, GB/T 50123—2019. 2019, Beijing, China.

Mondal, S., and Ghosh, A. (2019). Review on microbial induced calcite precipitation mechanisms leading to bacterial selection for microbial concrete. *Constr. Build. Mater.* 225, 67–75. doi:10.1016/j.conbuildmat.2019.07.122

Pacheco, V. L., Bragagnolo, L., Reginatto, C., and Thome, A. (2022). Microbially induced calcite precipitation (MICP): review from an engineering perspective. *Geotech. Geol. Eng.* 40, 2379–2396. doi:10.1007/s10706-021-02041-1

Peng, J., Cao, T. C., He, J., Dai, D., and Tian, Y. M. (2022). Improvement of coral sand with MICP using various calcium sources in sea water environment. *Front. Phys.* 10, 11. doi:10.3389/fphy.2022.825409

Peng, L., Shen, P., Poon, C. S., Zhao, Y., and Wang, F. (2023). Development of carbon capture coating to improve the durability of concrete structures. *Cem. Concr. Res.* 168, 107154. doi:10.1016/j.cemconres.2023.107154

Song, C. P., Wang, C. Y., Elsworth, D., and Zhi, S. (2022). Compressive strength of MICP-treated silica sand with different particle morphologies and gradings. *Geomicrobiol. J.* 39, 148–154. doi:10.1080/01490451.2021.2020936

Tang, C., Shi, B., Cui, Y., Liu, C., and Gu, K. (2012). Desiccation cracking behavior of polypropylene fiber–reinforced clayey soil. *Can. Geotechnical J.* 49 (9), 1088–1101. doi:10.1139/t2012-067

Wang, X. R., Li, C., Fan, W. H., and Li, H. Y. (2022). Reduction of brittleness of fine sandy soil biocemented by microbial-induced calcite precipitation. *Geomicrobiol. J.* 39, 135–147. doi:10.1080/01490451.2021.2019858

Xiao, Y., Wang, Y., Wang, S., Evans, T. M., Stuedlein, A. W., Chu, J., et al. (2021). Homogeneity and mechanical behaviors of sands improved by a temperature-controlled one-phase MICP method. *Acta Geotech.* 16, 1417–1427. doi:10.1007/s11440-020-01122-4

Xie, J., Tang, C., Yin, L., Lu, C., Ningjun, J., and Shi, B. (2019). Mechanical behavior of microbial-induced calcite precipitation (MICP)-treated soil with fiber reinforcement. *Chin. J. Geotechnical Eng.* 41, 675–682. doi:10.11779/CJGE201904010

Yin, L. Y., Tang, C. S., Xie, J., et al. (2019). Factors influencing the improvement of geotechnical material properties by microbial mineralization. *Geotechnics* 40, 2525–2546. doi:10.16285/j.rsm.2018.0520

Zhao, Q., Li, L., Li, C., Li, M. D., Amini, F., and Zhang, H. Z. (2014). Factors affecting improvement of engineering properties of MICP-treated soil catalyzed by bacteria and urease. *J. Mater. Civ. Eng.* 26, 10. doi:10.1061/(asce)mt.1943-5533.0001013

Zhao, Y., Xiao, Z. Y., Fan, C. B., Shen, W. Q., Wang, Q., and Liu, P. H. (2020). Comparative mechanical behaviors of four fiber-reinforced sand cemented by microbially induced carbonate precipitation. *Bull. Eng. Geol. Environ.* 79, 3075–3086. doi:10.1007/s10064-020-01756-4

Zheng, J. J., Song, Y., Lai, H. J., et al. (2019a). Experimental study on the shear behavior of fiber-reinforced bio-cemented sand. *J. Civ. Environ. Eng.* 41 (1), 15–21. doi:10.11835/J.issn.2096-6717.2019.002

Zheng, J. J., Song, Y., Wu, C. C., et al. (2019b). Experimental study on mechanical properties of basalt fiber reinforced micp-treated sand. *J. Huazhong Univ. Sci. Technol. Sci. Ed.* 47 (12), 73–78. doi:10.13245/j.hust.191213

Zheng, Z., Sun, Y., Pan, X., and Zhang, L. (2023). Failure mechanism of fiber-reinforced prestressed concrete containments under internal pressure considering different fiber types. *Materials* 16 (4), 1463. doi:10.3390/ma16041463